ADVANCED SURFACE TREATMENTS AND ADHESIVE BONDING TESTING SCHEMES OF CERAMIC ASSEMBLIES

Andres Bujanda*, Aaron Forster[1], Wendy Kosik, Robert Jensen, Steven McKnight
Materials Division
Weapons and Materials Research Directorate
U.S. Army Research Laboratory
Aberdeen Proving Ground, MD, 21005

[1]Current address: National Institute of Standards and Technology
Gaithersburg, MD, 20899

ABSTRACT

Evaluation of bond strength between dissimilar materials such as those in ceramic-metallic systems has to date been qualitative, offering no quantitative comparative results. This was due primarily to the difficulties inherent in handling and machining brittle materials such as ceramics. In this study a testing scheme was developed to circumvent the mechanical property inconsistencies of a metallic-ceramic system and allow quantitative evaluation of bond strength in a titanium/alumina composite system. Using a carefully designed half-wedge configuration, results are compared to a standard full-wedge test and show comparable bond strength and strain energy release rate values. Additionally, the effects of surface treatments on the ceramic-metallic bond strength are also evaluated with the half-wedge configuration as well as the effects of surface treatment on the mechanical integrity of the alumina ceramic.

1. INTRODUCTION

Lightweight ceramic based armors (e.g. composite integral armors) have been proposed as candidate materials to meet ballistic and structural performance requirements of emerging Army Future Combat Systems (FCS). In these types of armor systems, a ceramic tile strike face, with the primary purpose of defeating the incoming projectile, is adhesively bonded to a fiber reinforced composite or metal backing plate, which serves as a structural member. To maintain ballistic and structural integrity of a composite integral armor package, particularly during multi-hit ballistic events, maximum adhesive bond strength and durability must be maintained between the ceramic and the backing plate. While adhesive bonding of metallic and composite substrates has been widely studied and is well known, such studies for ceramic materials have not been sufficiently documented.

1.1 Evaluating Ceramic Bond Strength

There are several available methods to create stronger interfacial bonds [Kono, 2001; Mittal, 2000]. Silane or other adhesion promoters coupled with structural adhesive formulations tailored for specific applications have vastly improved the performance of bonded assemblies. However, an adhesive bond that performs well in dry conditions may deteriorate rapidly under wet conditions at moderately high temperatures. Strong, durable bonds are required for adhesive bonding of multiple dissimilar materials, such as ceramics and metals. Certain components present hydrophilic interfaces that may accelerate bond degradation compared to polymer interfaces without a driving force for separation during exposure to hot-wet conditions. While these aspects of adhesion are well understood for metals and composites, the interactions of common adhesion promoters, such as silane coupling agents, have not been explored in the case of ceramic substrates.

Performing an adhesive bonding study using brittle ceramics as a substrate presents unique experimental challenges, as these types of materials are extremely difficult to machine into standard ASTM sample geometries. Measuring the uniaxial tensile strength of a ceramic directly is possible using a cylindrical or rectangular dog-bone specimen. However, specimen machining is costly and is especially difficult along the gage length and in the transition sections between gage and grip areas. Failures during testing can occur at transition sections and at the grips, invalidating results. Also, due to the relatively high stiffness of ceramics, alignment must be extremely precise to ensure that bending and other stress states do not cause premature failure of the specimens [Lawn, 1993]. These experimental difficulties are also pronounced for adhesion testing using ceramic substrates. Common adhesion testing configurations, such as double cantilever beam or single lap-shear joint, are prohibited and prevent the measurement of rigorous adhesive fracture energies. Most published literature related to polymeric adhesive-ceramic bonding has focused on bonding of dental

Report Documentation Page

Form Approved
OMB No. 0704-0188

1. REPORT DATE	2. REPORT TYPE	3. DATES COVERED
01 NOV 2006	**N/A**	**-**

4. TITLE AND SUBTITLE	5a. CONTRACT NUMBER
Advanced Surface Treatments And Adhesive Bonding Testing Schemes Of Ceramic Assemblies	5b. GRANT NUMBER
	5c. PROGRAM ELEMENT NUMBER
6. AUTHOR(S)	5d. PROJECT NUMBER
	5e. TASK NUMBER
	5f. WORK UNIT NUMBER
7. PERFORMING ORGANIZATION NAME(S) AND ADDRESS(ES) **Materials Division Weapons and Materials Research Directorate U.S. Army Research Laboratory Aberdeen Proving Ground, MD, 21005**	8. PERFORMING ORGANIZATION REPORT NUMBER
9. SPONSORING/MONITORING AGENCY NAME(S) AND ADDRESS(ES)	10. SPONSOR/MONITOR'S ACRONYM(S)
	11. SPONSOR/MONITOR'S REPORT NUMBER(S)

12. DISTRIBUTION/AVAILABILITY STATEMENT
Approved for public release, distribution unlimited

13. SUPPLEMENTARY NOTES
See also ADM002075., The original document contains color images.

14. ABSTRACT

15. SUBJECT TERMS

16. SECURITY CLASSIFICATION OF:			17. LIMITATION OF ABSTRACT	18. NUMBER OF PAGES	19a. NAME OF RESPONSIBLE PERSON
a. REPORT	b. ABSTRACT	c. THIS PAGE			
unclassified	**unclassified**	**unclassified**	**UU**	**8**	

ceramics and reports only qualitative experimental techniques. [Blatz, 2003; Taylor, 1994; Kern, 1998]

1.2 The Half-Wedge Configuration

1.2.1 Geometry Considerations

The half-wedge methodology was similar to the mica experiments conducted by Obreimoff in the 1930's. In this method a single compliant adherend was bonded to a stiff adherend. A half-wedge was inserted between the two adherends, and the energy supplied by the elastic bending of the compliant adherend drives further crack propagation either cohesively in the adhesive or interfacially along one of the interfaces. (Figure 1) The half-wedge geometry was an extreme example of asymmetric full-wedge tests that have become increasingly popular in the last few years. In contrast to almost all of the asymmetric full wedge tests, the configuration used in this study, however, utilizes dissimilar materials as adherends.

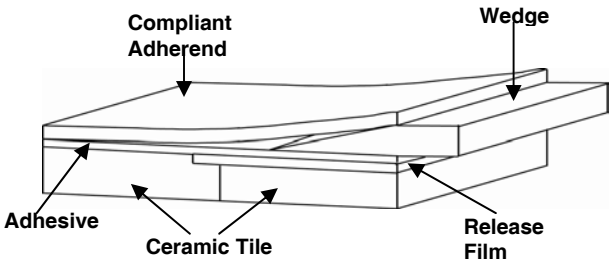

Figure 1. Schematic of the ½ wedge configuration.

1.2.2 Mode Mixity of Loading

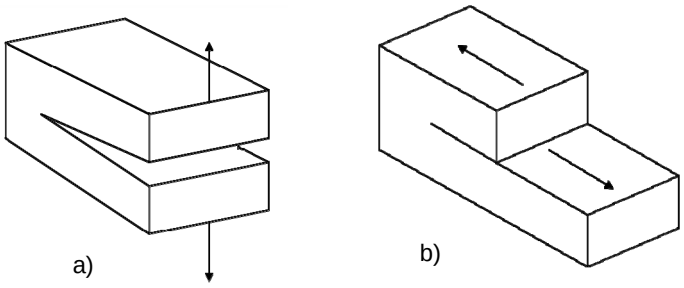

Figure 2. Schematics illustrating fundamental modes of failure in the ½ wedge: a) Mode I crack opening and b) Mode II in-plane shear.

Double cantilever beam (DCB) specimens are typically associated with pure mode I loading (Figure 2a). Asymmetric geometries provide an avenue for introducing mode II loading (Figure 2b) to the system. The mode mixity of asymmetric systems allows for testing adhesive bonds in conditions that may more closely resemble actual service stress conditions. Adhesives often have higher strengths in shear than in tension and modes of failure may vary depending on loading geometry. As the system becomes increasingly asymmetric a greater degree of mode II loading is introduced into the system.

The half-wedge configuration is the upper bound for mixed mode I and II loading, where some 38% of the energy was felt as in plane shear. (Figure 3) Mixed mode loading has also been shown to bias crack growth toward the interface of the stiffer adherend. The strain energy release rate, G, for the half-wedge configuration is given by the following expression.

$$G = G_I + G_{II} = \frac{3Eh^3}{8a^4}\Delta^2,$$

$$G_I = 0.6222G, G_{II} = 0.3778G$$

Where, E is the modulus of the compliant adherend, h is the thickness of the compliant adherend, Δ is the displacement at the loading point, and a is the crack length from the loading point [Tada, 2000].

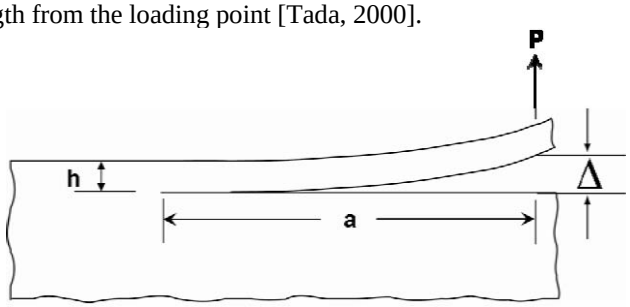

Figure 3. Fracture mechanics model of the asymmetric ½ wedge set-up.

1.3 Ceramic Strength Considerations

The strength of ceramic materials is largely governed by strength-limiting flaws, which can be introduced in the material during one of many stages of pre-processing, densification, or subsequent surface machining. There is a significant amount of post-processing handling of the ceramics used as structural components of composites. These include cleaning regiments, surface treatments, and heating and cooling cycles, all of which can effect the strength of the material by significantly altering an existing flaw population or by creating a new, dominant flaw population. Due to the high strength and low fracture toughness of ceramic materials, flaw tolerances are often extremely small, often on the order of a few microns. In addition to surface damage, examples of internal flaw populations include pores caused by incomplete densification, agglomerates of secondary phases, and excessively large primary phase grains [Green, 1998]. Determining the effects of the various surface treatments necessary for optimization of bond strength on the strength of the ceramic substrate itself was

possible by tracking changes in strength and fracture characteristics.

2. EXPERIMENTAL

2.1 Materials

Coorstek AD 995 alumina (Al_2O_3) was chosen for the ½ wedge adhesive bond test and for flexural strength evaluation. The alumina was machined into rectangular tiles with dimensions of 4 × 4 × 1 in for the ceramic adherend component. These tiles were further machined into 0.12 × 0.16 × 1.97 in rectangular bars for flexural strength testing. 120 flexure bars were machined out of the alumina for strength testing. The adhesive used was FM-94 film adhesive manufactured by Cytec, and the compliant adherend was a Ti6Al4V alloy machined into 8 × 1 × 1/8 in. strips. A ½ in aluminum backing plate bonded to the ceramic tile was used to keep the entire assembly in place during processing and testing. Four ½ wedge assemblies were constructed for the study, using a total of twelve alumina tiles. Two different surface preparations were evaluated in this investigation: acetone rinse (AT), AT and grit blast (GB). The effects of the various surface treatments were analyzed using X-Ray photoelectron spectroscopy (XPS).

2.2 Methods

The fabrication of the ½ wedge test sample was a multi-step process due to the difficulty in handling and bonding ceramic materials to dissimilar materials. Care was taken to ensure that stresses generated by thermal expansion coefficient mismatches between the different materials were not sufficient to cause failure during processing. Due to the stresses necessary to initiate and propagate a crack in this configuration, it was necessary for two tiles to be used per assembly. After processing, wedges were inserted into the adhered interfaces to initiate crack growth. The ½ wedge assemblies were placed in 65°C water in order to accelerate crack growth, and crack length was recorded for each assembly. Flexural strength was measured for the alumina at various stages of ceramic surface preparation and compared to the strength of the as-machined state.

2.2.1 The ½ -Wedge Test Sample Fabrication

2.2.1.1. Step 1 – Adhesive bonding of Al_2O_3 Tiles to Al Backing Plate

A ½ in aluminum backing plate was necessary to support the entire ½ wedge assembly. To ensure good bonding between the tiles and the aluminum, one side of the ceramic tiles as well as the aluminum plate were degreased using acetone, grit blasted with clean 180 grit white aluminum oxide grit, blown with nitrogen gas, and pretreated using a 1% (by weight) aqueous solution of 3-glycidoxypropyltrimethoxysilane (GPS). The two ceramic tiles and aluminum backing plate were bonded using two layers of FM94 epoxy film adhesive and cured under vacuum pressure at 250 °F for 1 hr. Two layers of adhesive were required to prevent the ceramic tiles from cracking upon cool down due to the mismatch of the constituents' coefficients of thermal expansion.

2.2.1.2 Step 2 – Surface Preparation of Titanium and Al_2O_3 Adherend Surfaces

Several different surface preparation procedures were conducted to examine the effect of surface treatment on bond strength using the ½ wedge configuration. Surface preparation included cleaning procedures, silane coupling agent application, and surface drying. For surface cleaning, samples were degreased with an acetone rinse and grit blasted with 180 grit alumina powder. Two of the specimens were only acetone washed. Two of the assemblies were acetone washed and then grit blasted.

An AC-130 sol-gel mixture was applied to all four samples using a laboratory spray bottle. The sample surface was kept wet for 2 min. The surfaces sol-gel treated ceramic tiles were blown dry using a high pressure (60 psi) stream of nitrogen gas from a cylinder. The nitrogen stream was directed along the length of the wedge test starting from the bonded end to the nonbonded end. This insured that any irregularities in the silane coating due to the drying process would be covered by the Kapton tape release liner.

After the sol-gel treatment, two of the ceramic assemblies were treated with a primer to further enhance bond strength between the ceramic and the FM-94. Again, the primer was left on for a few minutes and then blown dry using a high pressure (60 psi) stream of nitrogen gas from a cylinder.

2.2.1.3 Step 3 – Bonding of Titanium Adherends to Alumina Tiles

Following the surface treatment of the top side of the Al_2O_3 tiles, a thin layer of Kapton tape was applied to one of the ceramic tiles to prevent bonding and aid the insertion of the 1/2 wedge during subsequent testing. The titanium strips were then bonded to the treated ceramic tile surface using two strips of FM-94. The dimensions of the titanium strips allowed for three separate strips per assembly. Each one of these bonded strips was treated as an individual bonded joint, allowing three valid tests per sample condition. The ceramic/aluminum plate assembly with the titanium bonded to the top was then sealed in vacuum bagging film and placed under a vacuum pressure of ~1 atmosphere to ensure adequate contact of the bonded surfaces. The entire vacuum bagged assembly

was placed in an oven and the FM94 epoxy film adhesive was cured at a temperature of 250 °F for a period of 2 hr.

2.2.2 Bond Durability Studies Using the ½ Wedge Configuration

Once the complete titanium/ceramic 1/2 wedge test assembly is fully prepared the aluminum back plate is mounted to a framing fixture, which allows a stable clamping point to hold the fixture upright in a hydraulic press. The hydraulic press is used to slowly insert the 1/2 wedges to induce crack growth at the adhesive interface between the titanium adherend and the ceramic tile. The 1/2 wedges were fabricated from glass reinforced composite using an angle cutter mounted to a milling machine. The 1/2 wedges dimensions were 1 × 2 × 0.25 in with roughly a 45° angle cut at one end.

For hot/wet durability testing, the 1/2 wedge is inserted to a fixed loading point displacement and held constant. These samples are then placed into an environmental chamber for hot/wet conditioning. For each surface preparation condition of AT/SG and AT/GB/SG, six 1/2 wedge test samples (note: 3 samples per 1 assembly) were placed into a container of warm water (100% relative humidity) at a temperature of 140 °F. The samples were periodically removed for short times to measure the crack lengths. Figure 4 shows a completed assembly.

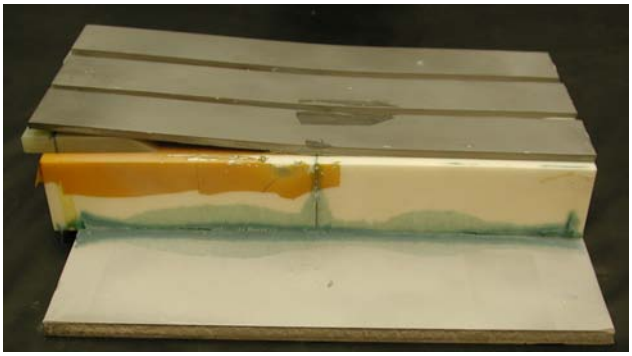

Figure 4. Completed ½ wedge specimen showing Ti6Al4V bonded to AD 995 alumina with FM-94 film adhesive.

2.2.3 XPS Analysis of Alumina Surface Chemistry

To examine the effects of surface preparation to the ceramic, rectangular AD-995 specimens ½ × ½ × ¼ in dimension were subjected to AT, AT/GB, and AT/GB/SG surface treatments. XPS analysis of the alumina specimens was performed after each cleaning step and after each silane treatment.

A Kratos Ultra XPS system, equipped with a hemispherical analyzer, characterized the near surface composition of the Al_2O_3 substrate and as deposited SG/SiC substrate. A 196W monochromatic Al Kα (1486.7eV) beam irradiated 1 × 1/2 mm spot. All spectra were taken at a 2×10^{-9} torr vacuum environment or better. Survey and elemental high resolution scans were taken at pass energy = 80eV for 2 min and pass energy = 20 eV for 2–8 min depending on S/N, respectively. The photoemission spectra allow quantitative (surface concentrations) and qualitative (functional group identification) information to be obtained. A hybrid electrostatic and magnetic lens column with an integral coaxial charge neutralizer was employed to maintained uniform surface charge for the exact spot under examination. Kratos' VISION2 software was utilized for all data analysis.

2.2.4 Flexural Strength Evaluation of Surface Treated Alumina

An investigation was designed in order to determine the effects of grit blasting on the strength and integrity of ceramic materials utilized in composite armor panels. Flexural strength testing was conducted on the alumina in accordance with. ASTM C1161. The standard "B" size specimen was used (0.12 × 0.16 × 1.97 in). There were four different sets of samples tested in this experiment; AT, AT/GB, AT/GB/SG, and AT/GB/SG/FM94. It was expected that the strength of the alumina would drop as a result of the damage caused by the abrasive grit blasting. It has also been observed that the tensile strength of glass fibers often increases once a sizing is applied, presumable due to a crack healing effect. It was hypothesized that once the grit blasted alumina was treated with a silane or sol-gel treatment and the film adhesive was cured to the surface that the damaging effects of the grit blasting medium could possibly be negated due to similar crack healing mechanisms. Therefore, the as-received and grit blasted alumina bend bars were subsequently treated with AC-130 sol-gel and bonded to FM94 film adhesive using procedures similar to those outlined previously in this paper. The FM94 was bonded to a single side of the bend bars (the grit blasted side for the GB samples) using a heated press at 250 °F for 2 hr. The pressure of the press was adjusted to mimic the vacuum pressures encountered during the vacuum assisted resin transfer molding (VARTM) processing of an assembled armor package. Thirty valid four-point flexural strength tests for each surface preparation were conducted on an Instron universal testing frame. Fractography was conducted on failed specimens to more accurately capture the intrinsic flaw population in the as-received samples and the strength-dominating flaw population for each of the different surface treatments. A Philips FEI Quanta environmental scanning electron microscope was used for fractography.

2.3 Results and Discussion

2.3.1 Bond Durability Studies Using ½ Wedge Configuration

The bond durability studies conducted using the ½ wedge configuration proved to be a viable and comparable method to the more common full wedge and lap shear evaluations. The average fracture energy imputed by the insertion of the wedge was 2027 ± 176 J/m^2. The amount of crack growth for each specimen was measured daily over the course of three weeks of immersion in the 140°F water. Figure 5 shows the average amount of crack growth for the AT and AT/GB specimens. The points on the figure highlighted with green indicate samples that completely failed during that testing interval. For the samples that were acetone rinsed only, crack lengths were significantly greater than AT/GB specimens for the entire duration of testing. After the first day of testing, for example, the average crack length for the AT specimens was 33 mm, while it was only 7.5 mm for the AT/GB specimens. The difference in crack length between the two sample sets (26 mm) was maintained for much of the experiment. This indicates that similar crack growth patterns are maintained across different surface preparations.

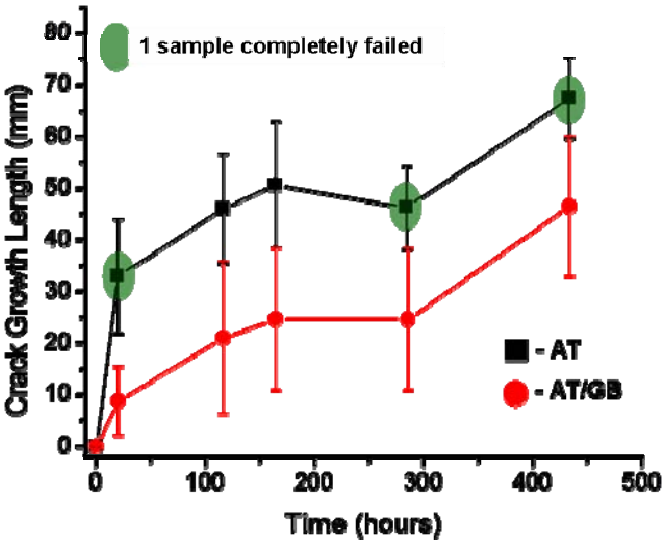

Figure 5. Average crack growth for ½ wedge specimens tested in 140°F water. Specimen surfaces were either acetone rinsed (AT) and acetone rinsed and grit blasted (AT/GB).

After 433 hours of testing, all specimens that had not failed were manually failed in order to discern the type of failure exhibited at the ceramic/adhesive interface. Figure 6 shows three specimens for a) AT and b) AT/GB surface preparations including the ceramic adherend (left) and the titanium adherend (right). The failure due to manual overload is indicated by the cohesive failure region where the FM94 adhesive is still visible on both adherends. The region of crack growth due to the insertion of the ½ wedge was marked by adhesive failure at the ceramic/FM94 interface. This indicated that the ½ wedge configuration evaluates the bond strength of the ceramic/adhesive bond and not the strength of the adhesive itself.

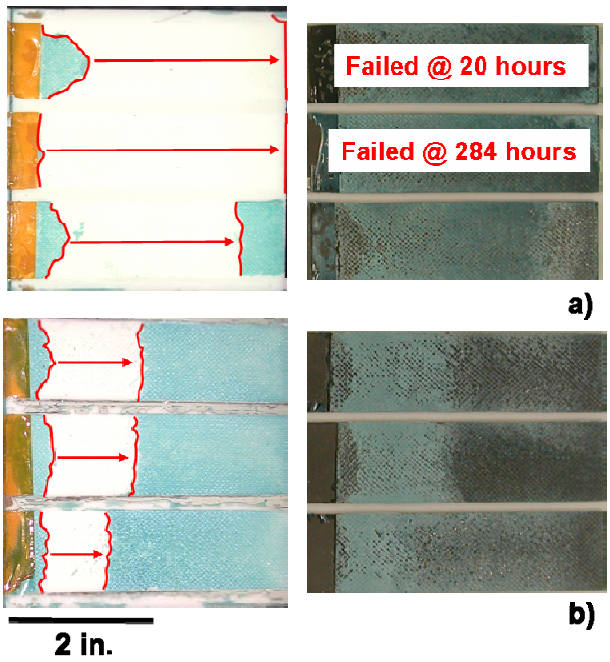

Figure 6. Photographs of manually failed ½ wedge specimens after 433 hours of immersion. AT specimens (a) and AT/GB specimens are pictured. The white region (left) is the alumina adherend and the titanium (right) is the corresponding compliant adherend.

One can clearly see the difference in crack length between the AT and AT/GB surface preparations in Figure 6. In this particular AT sample (a), two of the three AT ½ wedge test specimens failed prior to the end of the test duration, while none of the AT/GB specimens (b) failed during immersion testing. This indicated that grit blasting was a necessary step for optimal bond strength.

2.3.2 XPS Analysis of Surface Treated Alumina

XPS analysis revealed that the surface preparation methods utilized to maximize bond strength (grit-blasting) have a pronounced effect on the surface chemistry of the ceramic substrate material. Grit blasting the ceramic surface is conducted to remove surface contamination. In particular, the abrasive wear caused by the grit blasting media acts to reduce the amount of adventitious carbon on the surface of the alumina. This allows the true alumina surface previously covered by the carbon to now bond with the silane coupling agent (GPS or sol-gel). This

maximizes the effectiveness of the silane coupling agent and results in stronger bond strength when the adhesive is cured on the surface. XPS data from alumina specimens subjected to an acetone wash only and acetone/grit blast regiments are shown in Figure 7. The carbon-aluminum ratio is an indication of how much carbon is present on the surface relative to alumina. A higher ratio indicates an excess of carbon. For the AT specimens, the carbon-aluminum ratio was 0.52. For the AT/GB specimens the ratio dropped to 0.26, indicating a significant decrease in the amount of carbon on the surface of the alumina.

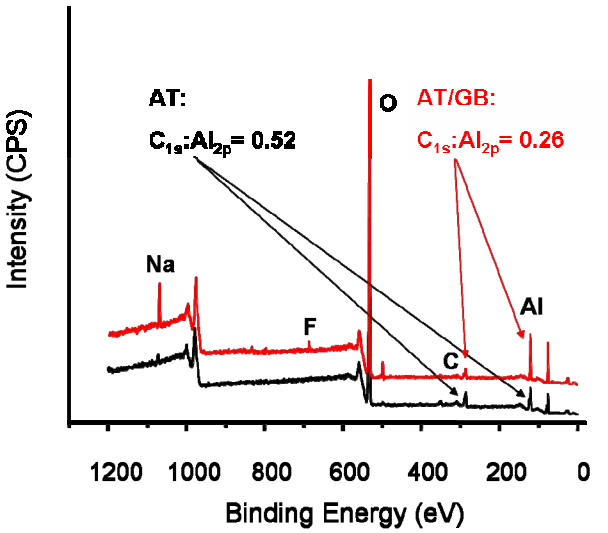

Figure 7. XPS results for different surface treatments of alumina bonding schemes.

2.3.3. Flexural Strength Testing Results

The effects of surface preparation on the alumina ceramic substrate were discerned from flexural strength testing. For the as-machined specimens, with a surface finish of 600 grit and were acetone washed, the characteristic strength was 291 MPa. The corresponding Weibull modulus was 42.0. Figure 8 is a Weibull plot of the AT and AT/GB strength data. The strength value was typical of similar alumina materials and the relatively high Weibull modulus indicates a low variability in strength distribution. From the Weibull distribution it is evident that there is only one dominant flaw population in the as-machined ceramic. ESEM fractography revealed the dominant flaw population to be surface machining damage (Figure 9). The semi-elliptical cracks observed intersecting the tensile surface of the specimen were caused by the abrasive nature of specimen machining. Fracture mechanics solutions and visual confirmation place the range of flaw sizes to be 105-133.8 µm.

For the AT/GB sample set, the characteristic strength drops to 282 MPa the Weibull modulus drops to 39.8 from the as-machined values (Figure 8). The ~3% decrease in strength was due to exacerbation of the pre-existing surface flaws observed in the as-machined specimens. The abrasive nature of grit blasting gives raise to tensile stress fields where the maximum stress is below the surface of the material. The stresses are relieved through the introduction of new surface defects or through growth in existing defects, both of which cause a decrease in the strength of the material. Fractography of the AT/GB specimens confirmed that existing surface defects had been exacerbated by the abrasive grit blast (Figure 10). Fracture mechanics calculations placed the range of strength-limiting defect size between 116.2-140.1 µm, confirming the observed trend.

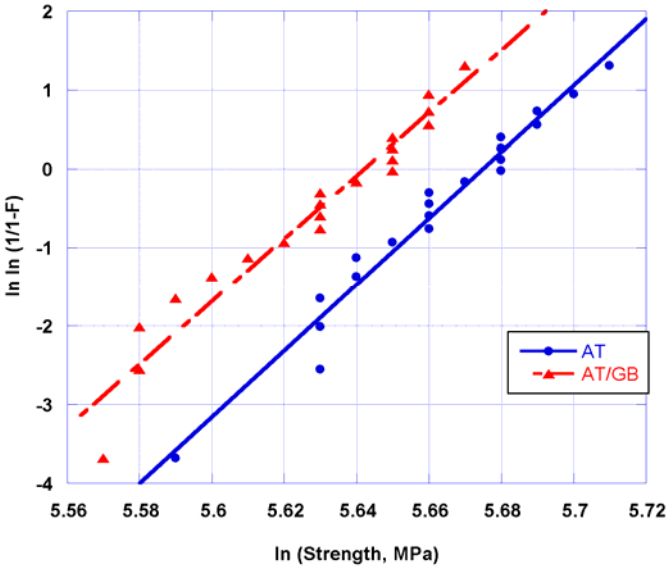

Figure 8. Weibull distribution for flexural strength of as-machined alumina subject to: 1) an acetone rinse (AT) and 2) an acetone rinse and grit blast.

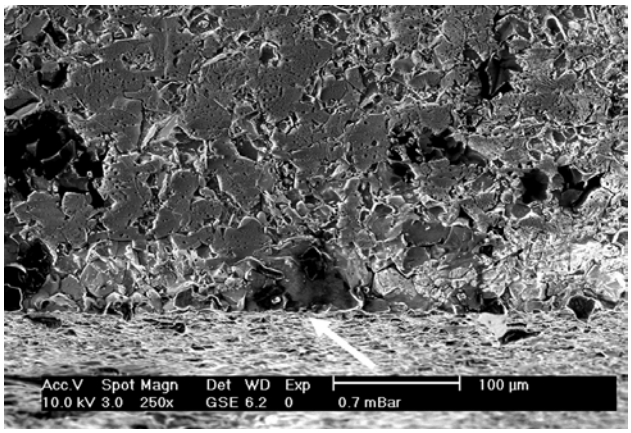

Figure 9. ESEM micrograph depicting the strength-limiting flaw in an AT alumina flexure specimen. The flaw, indicated by the white arrow is a sub-surface semi-elliptical crack induced by surface machining damage.

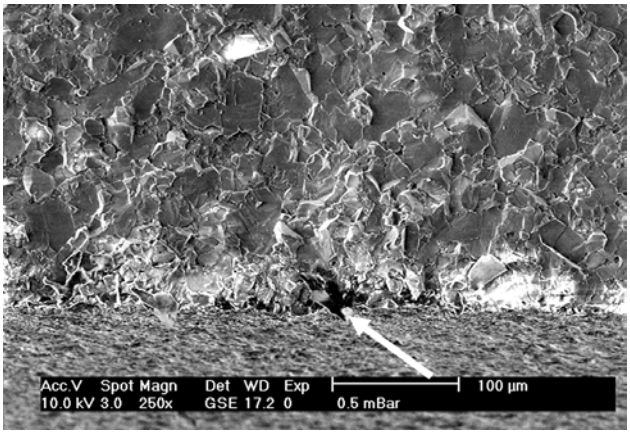

Figure 10. ESEM micrograph depicting strength-limiting surface machining damage in an AT/GB alumina flexure specimen. The white arrow indicates the origin of failure.

Flexural strength results for AT/GB and sol gel silane coupling agent treated specimens shows a marked "recovery" in strength. The characteristic strength and Weibull modulus of the AT/GB/SG sample set were 298.5 MPa and 32.2, respectively. FIGURE 11 shows the Weibull distribution for the AT/GB/SG specimens in comparison to the other sample sets. The characteristic strength of the AT/GB/SG alumina is slightly higher than the as-machined specimens, indicating that the sol-gel acts to suppress or negate not only the effects of the grit blasting, but affects the original flaw population as well. The exact mechanism for this strengthening is not known. However, it is hypothesized that the sol-gel acts to either reduce stress concentrations associated with surface asperities or enters the cracks and acts to shield the crack tips from the maximum stresses during loading.

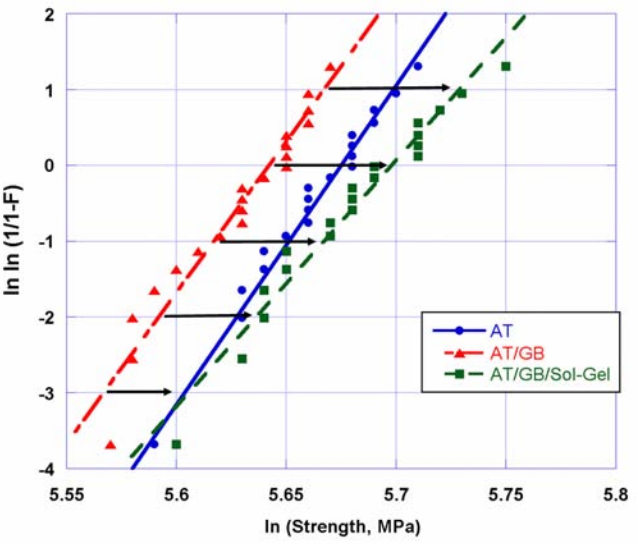

Figure 11. Weibull distribution for flexural strength of AT, AT/GB, and AT/GB/SG flexural strength specimens. Note the recovery in flexural strength of the AT/GB specimens when a sol-gel silane coupling agent was added to the tensile surface.

FM94 film adhesive was applied to the tensile side of alumina flexure bars that had been either acetone washed or acetone washed and grit blasted. Both sets of specimens were treated with the sol-gel silane coupling agent. The characteristic strength for both the AC/SG/FM94 and AC/GB/SG/FM94 was 350 MPa (Figure 12). The identical value of characteristic strength despite the different surface preparation regiment indicates that the flexural strength is significantly affected by the surface state of the ceramic material. The application of a silane coupling agent or a thin film adhesive acts to negate the effects of previous surface treatments including machining and grit blasting. Fractography of the FM94 coated flexure specimens revealed that failure still originated at surface machining defects, although failure from orthogonal machining cracks was observed in addition to cracks parallel to the machining direction (FIGURE 13). The surface coatings may suppress the dominant flaw population to the extent that a secondary population becomes active.

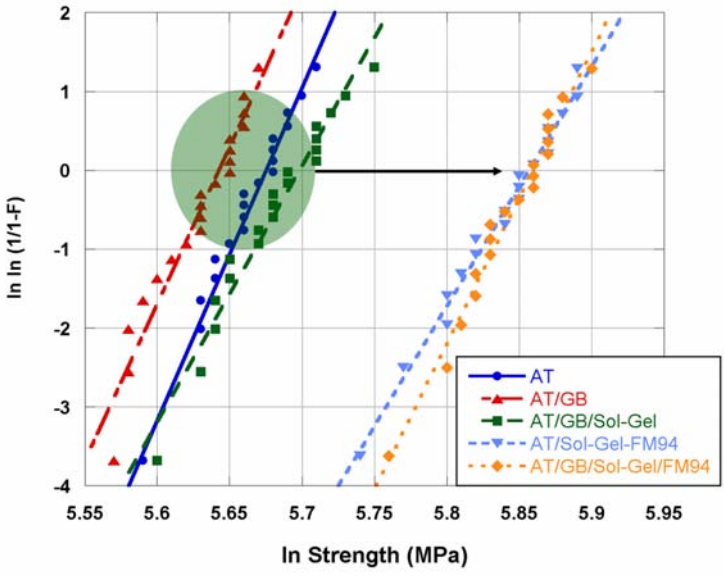

Figure 12. Weibull distribution for flexural strength of all alumina specimens. Note the increase in flexural strength when the film adhesive was applied to the tensile surface regardless of prior surface preparation.

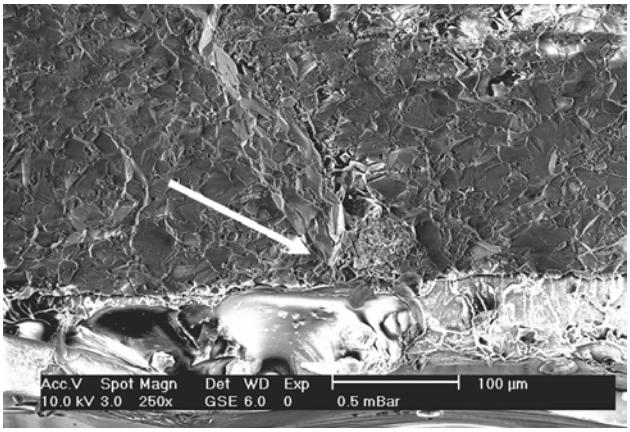

Figure 13. ESEM micrograph showing strength-limiting orthogonal surface machining crack in an alumina flexure specimen coated with a single layer of FM-94 film adhesive. The white arrow indicates the failure origin on the tensile surface.

3. CONCLUSIONS

This investigation was the first rigorous test utilizing the ½ wedge configuration to evaluate the bond strength between dissimilar materials. The ½ wedge design is sound and is applicable to a variety of material systems, though many aspects of mechanical mismatch between the different system constituents must be dealt with. The coefficient of thermal expansion mismatch was of particular importance for the alumina/titanium system used in this study.

The effects of different surface preparation techniques on bond durability were also successfully evaluated using the ½ wedge configuration. Differences in crack length between AT and AT/GB specimens were consistent throughout the three week evaluation period. These results were confirmed by XPS analysis. Cleaning with acetone alone does not remove adventitious carbon from the alumina surface. Abrasive surface cleaning by grit blasting with alumina particulates removes adventitious carbon, exposing the true alumina surface to bond with coupling agents. This results directly in an increase in bond strength and durability

Grit blasting the surface of a ceramic in order to optimize bond strength lowers the flexural strength of the material. However, the application of surface agents such as sol-gel or adhesive film counters the negative strength effects of surface preparation. In addition, flexural strength of the SG and FM-94 specimens was higher than the as-machined specimens, indicating that the coatings act to reduce the effectiveness of the dominant surface flaw population.

REFERENCES

Blatz, M. B., Sadan, A. Kern, M., 2003: Resin Ceramic Bonding: A Review of the Literature. *J. Prosthetic Dentistry*, **89**, 268-274.

Green, DJ, 1998: *An Introduction to the Mechanical Properties of Ceramics.* Cambridge University Press, 328 pp.

Kern M., Wegner SM., 1998: Bonding to Zirconia Ceramic: Adhesion Methods and Their Durability. *Dental Materials*, **14**, 64-71.

Kono, M., Sun, X., Li, R. Wong, K. C., Mitchell, K. A. R., Foster, T., 2001: Characterization of Aluminum Surfaces After Different Pretreatments and Exposure to Silane Coupling Agents. *Surf. Rev. Lett.*, **8,** 43-50.

Lawn, Brian, 1993: *Fracture of Brittle Solids- Second Edition.* Cambridge University Press, 378 pp.

Mittal, KL, ed., 2000: *Silane and Other Coupling Agents.* VSP.

Tada, Paris, Irwin, 2000: *The Stress Analysis of Cracks Handbook- Third Edition.* ASME Press, 677 pp.

Taylor, A. M., Watts, J. F., Duncan, H., Fletcher, I. W., 1994: Interphase Formation and the Characterization of Polymer/Ceramic Adhesion. *J. of Adhesion,* **46,** 145-160.